



Cite this: *Dalton Trans.*, 2019, **48**, 8106

Stereoisomers and functional groups in oxidorhenium(v) complexes: effects on catalytic activity†

J. A. Schachner, * B. Berner, F. Belaj and N. C. Mösch-Zanetti *
DOI: 10.1039/c9dt01352k
rsc.li/dalton

The syntheses of oxidorhenium(v) complexes $[\text{ReOCl}(\text{L1a-c})_2]$ (**3a-c**), equipped with the bidentate, mono-anionic phenol-dimethyloxazoline ligands **H1a-c** are described. Ligands **HL1b-c** contain functional groups on the phenol ring, compared to parent ligand 2-(4,4-dimethyl-4,5-dihydro-1,3-oxazol-2-yl)-phenol **H1a**; namely a methoxy group *ortho* to the hydroxyl position (2-(4,4-dimethyl-4,5-dihydro-1,3-oxazol-2-yl)-6-methoxyphenol, **H1b**), or a nitro group *para* to the hydroxyl position (2-(4,4-dimethyl-4,5-dihydro-1,3-oxazol-2-yl)-4-nitrophenol, **H1c**). Furthermore, oxidorhenate(v) complexes (NBu_4) $[\text{ReOCl}_3(\text{L1a-b})]$ (**2a-b**) were synthesized for solid state structural comparisons to **3a-b**. All novel complexes are fully characterized including NMR, IR and UV-Vis spectroscopy, MS spectrometry, X-ray crystallography, elemental analysis as well as cyclic voltammetry. The influence of functional groups ($\text{R} = -\text{H}$, $-\text{OMe}$ and $-\text{NO}_2$) on the catalytic activity of **3a-c** was investigated in two benchmark catalytic reactions, namely cyclooctene epoxidation and perchlorate reduction. In addition, the previously described oxidorhenium(v) complex $[\text{ReOCl}(\text{oz})_2]$ (**4**), employing the phenol-oxazoline ligand 2-(4,5-dihydro-2-oxazolyl) phenol **HoZ**, was included in these catalysis studies. Complex **4** is a rare case in oxidorhenium(v) chemistry where two stereoisomers could be separated and fully characterized. With respect to the position of the oxazoline nitrogen atoms on the rhenium atom, these two stereoisomers are referred to as *N,N-cis* and *N,N-trans* isomer. A potential correlation between spectroscopic and structural data to catalytic activity was evaluated.

Received 29th March 2019,
Accepted 17th April 2019
DOI: 10.1039/c9dt01352k
rsc.li/dalton

Introduction

The interest in the chemistry of high oxidation state rhenium oxides was certainly triggered by the two seminal publication on methyltrioxorhenium(vii) (MTO) by Herrmann in 1991.¹ After finding an elegant synthesis of MTO, the group of Herrmann and others demonstrated the impressive catalytic activities in oxidation catalysis by MTO, including catalytic epoxidation of a wide variety of olefins.^{2,3-5} To this day, MTO remains the most active rhenium-based epoxidation catalyst, reaching turnover numbers (TONs) of $>20\,000$.^{3,6,7} However, MTO suffered from epoxide hydrolysis, when acid-sensitive epoxides are formed.⁸ This observed drawback, as well as decomposition reactions of MTO, prompted the investigation of oxidorhenium(v) complexes as potential epoxidation cata-

lysts. The first two examples of such rhenium(v) complexes again came from the group of Herrmann, using tetra- and bidentate Schiff-base ligands.^{9,10} Over the last few years the chemistry of oxidorhenium(v) complexes and their application in homogeneous catalytic epoxidation of cyclooctene further developed.^{6,11-18} Compared to the impressive activities of MTO however, oxidorhenium(v) complexes had been inferior epoxidation catalysts, with the published complexes until 2014 only reaching turnovers of $\text{TON} < 75$.¹⁷ Our initial research efforts concentrated on phenol-pyrazole (HpyzR) ligands, equipped with various substituents R ($\text{R} = \text{H, Me, OMe, Br, NO}_2$) on the phenol moiety (Fig. 1).^{14,16}

The introduction of functional groups on the phenol moiety was found to have a beneficial effect on epoxidation activity of the resulting oxidorhenium(v) complexes $[\text{ReOCl}(\text{pyzR})_2]$.¹⁴ Especially the set of complexes with $\text{R} = \text{OMe, Br}$ and NO_2 showed enhanced activities ($\text{TON} > 95$) in the epoxidation of cyclooctene (1 mol% cat. loading, 3 equiv. TBHP) as well as activity with the green oxidant H_2O_2 (TONs between 55 to 61).¹⁴ In contrast, complexes $[\text{ReOCl}(\text{pyzR})_2]$ with $\text{R} = \text{H}$ and Me showed either reduced epoxidation activity ($\text{TON} < 60$, with TBHP) or none at all ($\text{TON} = 0$, with H_2O_2) under the same con-

Institute of Chemistry, University of Graz, Schubertstr. 1, 8010 Graz, Austria.
E-mail: joerg.schachner@uni-graz.at

† Electronic supplementary information (ESI) available: Details on synthesis of ligand **H1c** as well as crystallographic data of complexes **2a-b** and **3a-c**. CCDC 1895410, 1850856 and 1562677-1562679. For ESI and crystallographic data in CIF or other electronic format see DOI: 10.1039/c9dt01352k



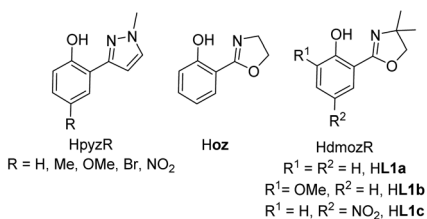


Fig. 1 Phenol-pyrazole and phenol-oxazoline *ON*-bidentate ligands used in oxidorhenium(v) chemistry, shown with their commonly used abbreviations.

ditions.¹⁴ Whereas MTO and related oxidorhenium(vii) complexes were shown to form side-on coordinated mono-peroxy and bis-peroxy complexes as the active catalyst,^{4,5,18,19} no such structures have been observed or isolated for oxidorhenium(v) complexes like **3a–c**. A peroxide activation mechanism *via* deprotonation of the incoming peroxide similar to dioxidomolybdenum(vi) complexes²⁰ seems less likely for oxidorhenium(v) complexes. Here, the oxido ligand is much less nucleophilic due to strong π -bonding.²¹

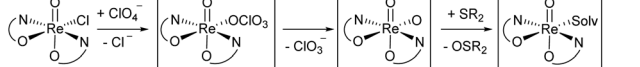
A second type of catalytic reaction effected by an oxidorhenium(v) complex was first described in 2000. The group of Abu-Omar reported the capability of complex $[\text{ReOCl}(\text{oz})_2]$ (**4**), equipped with the phenol-oxazoline ligand **Hoz** (Fig. 1), to catalytically reduce perchlorate anions to chloride.^{22–24} We also became interested in this remarkable chemistry of the **Hoz** ligand, and began to investigate the oxazoline-dimethyl version of the **Hoz** ligand, the **Hdmoz** ligand (**HL1a**, Fig. 1), in perchlorate reduction chemistry.¹² Based on the ground laying work of the Abu-Omar group, a dissociative oxygen atom transfer (OAT) mechanism of redox-catalysis was postulated, with the Re atom cycling between Re(v) and Re(vii) (Scheme 1).^{22–25}

In perchlorate reduction catalysis, we could show that isomers play an important role for catalyst activity.^{11,12} For an octahedral complex with two ON-bidentate and two monodentate ligands like **3a–c**, six stereoisomers could form in principle (Scheme 2). Isomers A and B have a *trans* arrangement of the oxido and X ligand, with the bidentate ON-ligand in the

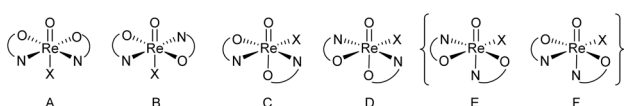
equatorial plane. Both isomers contain an element of symmetry (σ or C_2) and are therefore also referred to as “symmetric isomers”. Depending on the relative position of the nitrogen donor atom, isomer A is referred to as an *N,N-cis* isomer, B as an *N,N-trans* isomer. In isomers C to F, ligands O and X adopt a mutual *cis* orientation to each other, resulting in total loss of symmetry. Most of the isolated oxidorhenium(v) complexes belong to asymmetric isomers C and D.¹⁷ Again C constitutes an *N,N-cis* and D an *N,N-trans* isomer. Isomers E and F have not been observed yet in rhenium chemistry. This might be due to the strong *trans* influence of the oxido ligand, making the coordination of the neutral nitrogen donor in this position unlikely.

For parent complex $[\text{ReOCl}(\text{oz})_2]$ **4**, both the *N,N-cis* (C, *cis*-**4**) and *N,N-trans* (D, *trans*-**4**) isomer are formed in the synthesis (Scheme 4). It could be shown that *trans*-**4** is more active in perchlorate reduction compared to *cis*-**4**.¹² The initial step of the catalytic cycle is loss of the chlorido ligand, creating a vacant site on the rhenium atom. In *cis*-**4**, the neutral nitrogen atom of the oxazoline moiety is *trans* to the chlorido ligand, exerting a weaker *trans*-influence compared to *trans*-**4**, where the phenolate oxygen atom is *trans* to the chlorido ligand (Scheme 2). This situation elongates the Re–Cl bond in *trans*-**4** (2.4093(10) Å), compared to *cis*-**4** (2.383(3) Å).¹² Hence the loss of chlorido ligand requires less energy for *trans*-**4**. The same is true for the subsequent steps in the catalytic cycle. Those are OAT from the substrate to the rhenium atom and subsequent OAT from rhenium to the sulfide acceptor. For all these steps, the energy barriers are higher for *cis*-**4** compared to *trans*-**4**.¹² In the synthesis of complexes **3a–c**, special attention was paid on the potential formation of *N,N-cis* or *N,N-trans* isomers (Scheme 4), because of their significant influence on catalytic activity.^{12,22,26,27} Stereocontrol in the synthesis of oxidorhenium(v) complexes to obtain the desired *N,N-trans* isomer is therefore highly desired. In literature, it was shown that a single methyl group on the oxazoline moiety is sufficient for the isomerically pure formation of an *N,N-trans* isomer.^{26,27} The resulting steric hindrance in an hypothetical *N,N-cis* complex was identified as one source of stereo-control.²⁷ The observation that complexes *cis/trans*-**4**, without a substituent on the oxazoline moiety, are obtained as a mixture of *N,N-cis* and *N,N-trans* isomers supports this conclusion. Within this manuscript we would like to present an additional element of stereocontrol, based on the coordination chemistry of the **Hdmoz** ligands **HL1a–c**.

With this manuscript, we would like to present results obtained for the set of oxidorhenium(v) complexes $[\text{ReOCl}(\text{L1a–c})_2]$ in epoxidation and perchlorate reduction catalysis. By systematic introduction of electron-donating (–OMe, **HL1b**) and an electron-withdrawing (–NO₂, **HL1c**) groups (Fig. 1) we are relating structural and spectroscopic factors to catalytic activity. In addition factors that control the stereoselectivity of the synthesis of these complexes were investigated with the help of model complexes **2a–b**. Finally the influence of stereoisomerism on catalytic epoxidation activity was tested with complexes *cis*- and *trans*-**4**.



Scheme 1 Proposed dissociative oxygen atom transfer mechanism of perchlorate reduction via Re(v)/(vii) redox catalysis; solv = solvent.



Scheme 2 Possible stereoisomers A–F for octahedral $[\text{ReOX(ON)}_2]$ complexes (E and F have not been observed yet).



Results and discussion

Synthetic procedures

Ligands **HL1a–b** were synthesized according to literature,^{12,28,29} **HL1c** based on established literature procedures³⁰ with modifications (see ESI†). Anionic oxidorhenenate(v) complexes (NBu_4) $[\text{ReOCl}_3(\text{L1a–b})]$ **2a–b** were obtained by reaction of precursor complex (NBu_4) $[\text{ReOCl}_4]$ with one equivalent of ligand **HL1a** or **HL1b** at room temperature in EtOH (Scheme 3). Only this precursor, together with short reaction times (0.5–1 h) at room temperature, allows for isolation of mono-ligated complexes **2a–b**. Under the same reaction conditions, precursor $[\text{ReOCl}_3(\text{OPPh}_3)(\text{SMe}_2)]$ gives mixtures with bis-ligated complexes **3a** and **3b**, respectively.

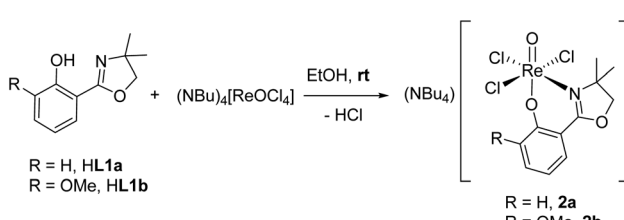
Complexes $[\text{ReOCl}(\text{L1a–c})_2]$ **3a–c** were obtained by reaction of precursor complex $[\text{ReOCl}_3(\text{OPPh}_3)(\text{SMe}_2)]$ with two equivalent of ligands **HL1a–c** respectively, under refluxing conditions in CH_3CN (Scheme 4). Complete dissolution of the poorly soluble precursor complex as well as a typical color change of the reaction mixtures to green (**3a** and **3c**) or greenish-brown (**3b**) indicate successful synthesis of the respective complexes. The isolated complexes are stable to air and moisture, and are in general insoluble in non-polar solvents like pentane or heptane. Based on their substituents on the phenol moiety, complex **3b** ($-\text{OMe}$) shows the highest solubility in polar solvents like CH_2Cl_2 , CHCl_3 , or CH_3CN , followed by **3a** ($-\text{H}$) and **3c** ($-\text{NO}_2$) with the lowest solubility. Also alcohols like CH_3OH and EtOH or $\text{CH}_3\text{CN}/\text{H}_2\text{O}$ mixtures are possible solvents. When using the HdmozR ligands **HL1a–c** in the synthesis of complexes **3a–c**, ^1H NMR spectroscopy and solid state

structural data obtained by single-crystal X-ray analyses (Fig. 3) confirmed the exclusive formation of *N,N-trans* isomers.

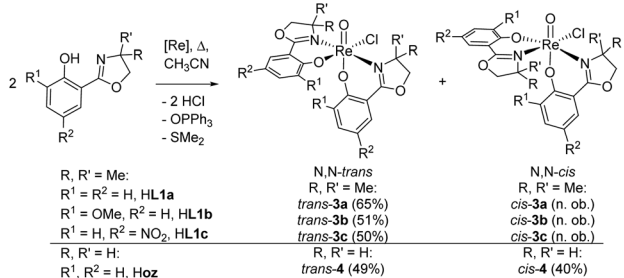
Crystallography

Single crystals for all five novel complexes **2a–b** and **3a–c** were obtained, and their solid state structure could be solved by X-ray crystallography. The molecular structures of **2a** and **2b** revealed the expected anionic oxidorhenenate(v) complexes with $(\text{NBu}_4)^+$ as counterion (Fig. 2). Both complexes adopt a slightly distorted octahedral conformation with similar bond lengths and angles (Table 1). The presence of the methoxy group in **2b** does not result in a significantly different coordination around the rhenium atom, compared to **2a**. Several other anionic trihalo oxidorhenenate(v) complexes have been structurally characterized and show the same coordination pattern.^{9,26,31–33} In all cases, the alkoxide oxygen of the ligand moiety coordinates *trans* to the oxido ligand, resulting in an axial-equatorial coordination of the bidentate ligand, with the three chlorido ligands in a meridional coordination. This preferred coordination might also explain the absence of isomers E and F (Scheme 2) in rhenium chemistry.

Single crystals of complex **3a** were obtained from an EtOH solution at 8 °C, of complex **3b** from an EtOH/EtOAc mixture at room temperature, and of complex **3c** from a saturated EtOH solution by slow evaporation at 8 °C. X-ray diffraction analysis revealed quite similar solid state structures, with the rhenium centers in a distorted octahedral coordination. In all



Scheme 3 Synthesis of $(\text{NBu}_4)[\text{ReOCl}_3(\text{L1a–b})]$ **2a–b**.



Scheme 4 Synthesis (isolated yield) of single isomer of *trans*-**3a–c** and isomeric mixture of complexes *cis/trans*-**4** ($[\text{Re}] = [\text{ReOCl}_3(\text{OPPh}_3)(\text{SMe}_2)]$; n. ob. = not observed).

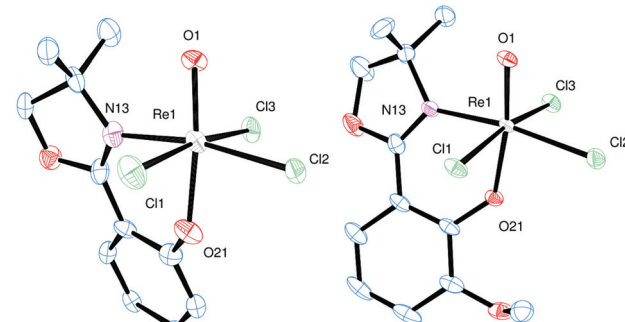


Fig. 2 Molecular views (50% level) of **2a** and **2b** (H atoms, solvent and $(\text{NBu}_4)^+$ molecules omitted for clarity).

Table 1 Selected bond lengths [Å] and angles [°] of **2a–b**

[Å]	2a	2b
Re1=O1	1.690(7)	1.6801(16)
Re1–N13	2.172(8)	2.1386(16)
Re1–O21	2.011(8)	1.9800(16)
Re1–Cl1	2.381(3)	2.3909(4)
Re1–Cl2	2.377(2)	2.3717(4)
Re1–Cl3	2.420(3)	2.3891(4)

[°]	2a	2b
O1–Re1–O21	171.4(3)	171.18(9)
Cl1–Re1–Cl3	171.51(10)	169.71(3)
N13–Re1–Cl2	169.7(2)	171.40(6)



cases the chlorido ligand is located *cis* to the oxido ligand. Furthermore, the *N,N-trans* orientation of the two bidentate ligands was confirmed for all three complexes (Fig. 3).

A summary of selected bond angles and distances for **3a–c** can be found in Table 2. The observed bond lengths in com-

plexes **3a–c** show that the solid state structures are sensitive to the substituents on the ligand moieties **L1a–c**. However, a clear trend is not easily extracted from the data at hand. For example, **3a** displays the longest Re–Cl1 distance, indicating a stronger *trans* influence of the **L1a** ligand moiety, compared to **L1b–c**. Also, complex **3a** displays the shortest Re=O bond, compared to complexes **3b–c**, which show comparable Re=O bond lengths, regardless of the electron-donating or -withdrawing nature of the phenol substituents. The rhenium-oxido and rhenium-chlorido bond lengths in **3c** are actually very similar to **3b**, equipped with the electron-donating ligand **L1b**.

Stereo-control of isomers

Switching from the Hoz to the Hdmoz ligand class, with two methyl groups on the oxazoline moiety, only leads to the respective *N,N-trans* complexes (Scheme 4). In order to study this stereoselective formation of *N,N-trans* isomers of **3a–c** in more detail, the two mono-ligated, anionic oxidorhenenate(v) complexes $(\text{NBu}_4)[\text{ReOCl}_3(\text{L1a})]$ (**2a**) and $(\text{NBu}_4)[\text{ReOCl}_3(\text{L1b})]$ (**2b**) were synthesized (Scheme 3). The formation of mono-ligated complexes **2a–b** provides evidence that the synthesis of bis-ligated complexes $[\text{ReOCl}(\text{L1a–c})_2]$ is a step-wise process. Thus, whether the *N,N-trans* or *N,N-cis* isomer is formed in the next step depends on the respective *trans* influence of the initially coordinated ligand moiety (Scheme 5).

Complex **2a** can be compared to previously published complex $(\text{H}_2\text{oz})[\text{ReOCl}_3(\text{oz})]$ (**2-oz**).²⁶ As mentioned above, the respective bis-ligated complex **3a** is isomerically pure, whereas **4** is isolated as an isomeric *N,N-trans* and *N,N-cis* mixture. As summarized in Table 3, for complex **2a**, the two *trans* co-ordinated chlorido ligands Cl1 and Cl3 exhibit longer bond distances to the Re center (2.381(3) and 2.420(3) Å, respectively) compared to chlorido ligand Cl2, which is *trans* to the oxazoline nitrogen N13. Here the Re–Cl bond distance is at

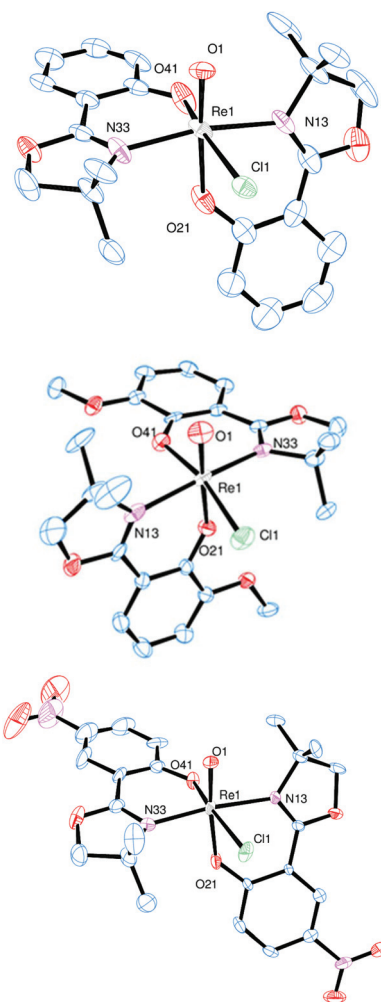


Fig. 3 Molecular views (50% probability level) of complex **3a** (top), **3b** (middle) and **3c** (bottom). Hydrogen atoms were omitted for clarity.

Table 2 Selected bond distances [Å] and angles [°] for complexes **3a–c**

[Å]	3a	3b	3c
Re1=O1	1.682(6)	1.757(4)	1.719(4)
Re1–Cl1	2.440(2)	2.400(2)	2.4087(18)
Re1–N13	2.203(5)	2.118(5)	2.205(3)
Re1–N33	2.058(5)	2.096(4)	2.037(3)
Re1–O21	2.056(7)	1.987(4)	2.033(3)
Re1–O41	1.944(7)	1.999(4)	1.962(3)
 [°]			
O1–Re1–O21	173.2(3)	177.3(3)	172.91(17)
Cl1–Re1–O41	163.8(6)	168.07(18)	166.62(10)
N13–Re1–N33	165.9(2)	165.4(3)	168.63(13)

Scheme 5 Schematic representation of step-wise coordination of a bidentate ligand H(ON) (e.g. **HL1a–c**), with formation of *N,N-trans* or *N,N-cis* isomers. Arrows indicate point of substitution of incoming phenolate oxygen of the second H(ON) ligand and resulting stereoisomer.

Table 3 Comparison of Re–Cl bond lengths [Å] of **2-oz**, **2a** and **2b**

	Re1–Cl1	Re1–Cl2	Re1–Cl3
2a	2.381(3)	2.377(2)	2.420(3)
2b	2.3909(4)	2.3717(4)	2.3891(4)
2-oz ²⁶	2.4701(6) ^a	2.3690(6)	2.3621(7)

^a Elongated because of H-bonding to neighboring $(\text{H}_2\text{oz})^+$ cations.



2.377(2) Å, as expected based on the weaker *trans* influence of N13. The same observations are made in case of **2b**, where bis-ligated complex **3b** also only shows the *N,N-trans* isomer. Complex **2-oz** displays an unusually long Re–Cl1 bond (2.4701(6) Å), which is caused by two H-bonds to neighboring (H_2oz)⁺ cations in the unit cell.²⁶ Therefore this bond has to be disregarded for the structural discussion. The remaining two bonds Re–Cl2 (2.3690(6) Å) and Re–Cl3 (2.3621(7) Å) are of very similar distances. Such a similar bonding situation could explain the observed mixtures of *N,N-cis* and *N,N-trans* isomers for **4**, as there is no preference for the point of coordination of the second incoming **Hoz** ligand (Scheme 5). The shorter and therefore stronger Re–Cl2 bonds observed in **2a** and **2b** would explain the stereoselective synthesis of *N,N-trans* complexes **3a–b**.

Cyclic voltammetry

In order to evaluate the electronic situation on the Re center with respect to the ligand substituents, cyclic voltammetry experiments on bis-ligated complexes **3a–c** were performed. In addition, also the two isomers of *N,N-cis/trans* **4** were investigated. Analyte solutions for cyclic voltammetry were near 1 mM in acetonitrile, with (NBu₄)PF₆ used as supporting electrolyte (0.1 M). The recorded currents I_p [μA] were divided by the actual concentration of analyte to normalize the voltammograms for better comparability. All five complexes displayed quasi-reversible Re(v)/vi redox couples at a positive potential,^{14,34} which also proved to be scan-rate independent. At negative potentials only irreversible redox events occurred. Half-wave potentials $E_{1/2}$ ($E_{1/2} = (E_{p,c} + E_{p,a})/2$) are given in Table 4 (referenced to ferrocene/ferrocenium).

For complexes **3a–c** (Table 4 und Fig. 4), the half-wave potential of **3c** is shifted by 280 mV to higher potential, compared to unsubstituted **3a**, as expected for the electron-withdrawing nature of the nitro groups on the ligand moiety of **L1c**. Methoxy substituted complex **3b** on the other hand is only shifted by 29 mV to lower potential, compared to **3a**, indicating a small electron-donating effect of the methoxy substituents in **3b**. The influence of the methyl groups on the oxazoline moiety can be compared between **3a** and *trans*-**4**. Here, the Re(v)/vi redox couple for *trans*-**4** is 60 mV lower than for **3a**, indicating an electron-richer metal center in *trans*-**4**. The data in Table 4 and Fig. 4 show that the two stereoisomer of **4** have virtually identical redox potentials. Obviously, stereoisomerism does not have an effect on the redox potential of the Re center.

Epoxidation of cyclooctene

Complexes **2a–b**, **3a–c** and *cis/trans*-**4** were evaluated as catalysts in the epoxidation of standard substrate cyclooctene. The

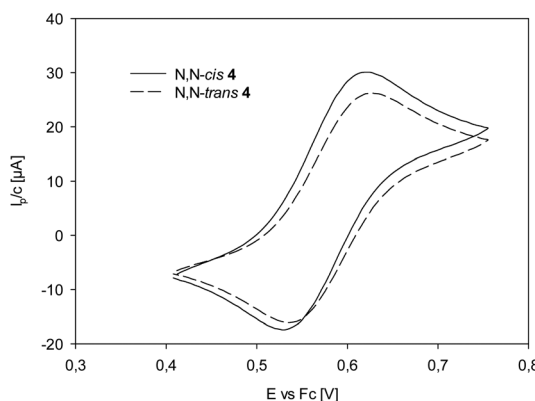
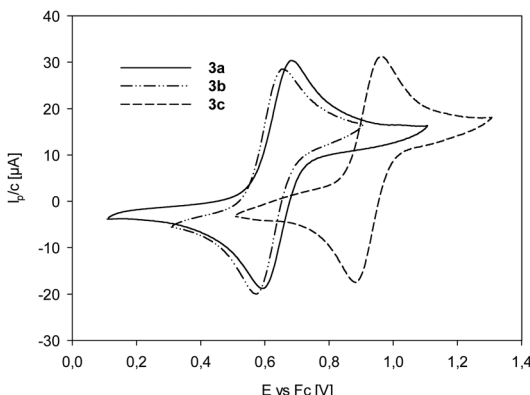
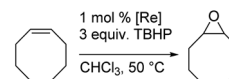


Fig. 4 Top: Comparison of Re(v)/Re(vi) redox couples of complexes **3a–c**; bottom: comparison of Re(v)/Re(vi) redox couples of complexes *cis/trans*-**4**.



Scheme 6 Epoxidation of cyclooctene using *tert*-butylhydroperoxide (TBHP).

effect of the different isomers *cis/trans*-**4** and the introduction of electron-donating (–OMe in **3b**) and withdrawing (–NO₂ in **3c**) groups on catalytic activity was of particular interest. Complexes **2a** and **2b** were also tested for potential catalytic activity, as other mono-ligated complexes have proven to be active epoxidation catalysts.^{14,15} In typical catalytic experiments 3 equiv. of *tert*-butylhydroperoxide (TBHP) as oxidant with a 1 mol% catalyst loading in CHCl₃ at 50 °C and the substrate cyclooctene were used (Scheme 6). Reaction progress was monitored by withdrawing aliquots during the reaction and analysis with GC-MS. In general, all six tested complexes are catalytically active without induction period. A summary of turnover numbers (TON) with the respective turnover frequency (TOF [h⁻¹]) is given in Table 5. The lowest activity was displayed by complex **2a**, the highest by **3c**. Complexes **3a** and **3b** showed activities in a similar range as *cis/trans*-**4**. All complexes tested showed a significant brightening to complete dis-

Table 4 Redox potentials $E_{1/2}$ [V] of complexes **3a–c** and *N,N-cis/trans* **4** at 200 mV s⁻¹ in CH₃CN

[V]	3a	3b	3c	<i>cis</i> - 4	<i>trans</i> - 4
$E_{1/2}$	0.642	0.613	0.922	0.576	0.582



Table 5 TON (TOF [h^{-1}]) for catalysts **2a–b**, **3a–c** and *cis/trans*-**4**

	TON (TOF)
2a	<10
2b	23 (0.96)
3a	37 (1.5)
3b^a	34 (1.4)
3c	80 (9.4)
<i>cis</i> - 4	40 (1.7)
<i>trans</i> - 4	30 (1.3)

TOFs [h^{-1}] were calculated at time of maximum yield of epoxide, not maximum activity of catalyst. If not mentioned otherwise, this was after 24 h. ^a Maximum yield of epoxide reached after 8.5 h.

coloration from the initially green solutions during catalytic experiments, hinting at the formation of catalytically inactive $\text{Re}(\text{vii})$ complexes.³¹

Time-conversion plots of cyclooctene epoxidation are given in Fig. 5.

Data in Fig. 5 and Table 5 show complexes **2a** and **2b** to exhibit the lowest activities (**2a**: TON < 10; **2b**: TON = 23) of all seven investigated complexes. The few examples of oxido-rhenate(v) complexes, that were also tested in epoxidation, were of similar low activity.^{31,33} Also the bis-ligated complexes **3a** (TON = 37) and **3b** (TON = 34) showed low activities in the epoxidation of cyclooctene. In the cases of complexes **2b** and **3b**, significant discoloration after addition of oxidant TBHP could be observed, indicating a fast oxidation to unproductive perrhenate(vii) salts.³¹ Hence, ligand **L1b** seems to result in unstable complexes under strong oxidative conditions. This is quite in contrast to the OMe-substituted pyrazole–phenol complex $[\text{ReOCl}(\text{pyzOMe})_2]$, which showed excellent activities in cyclooctene epoxidation for both TBHP and H_2O_2 .¹⁴ A potential reason for the lack of activity for **2b** and **3b** could be ring-opening or decomposition reactions of the non-aromatic oxazoline moiety in **L1b**, a known problem in oxazoline chemistry.²⁴ In contrast to **3b**, complex **3c**, coordinated by the electron-withdrawing ligand moiety **L1c**, showed the highest

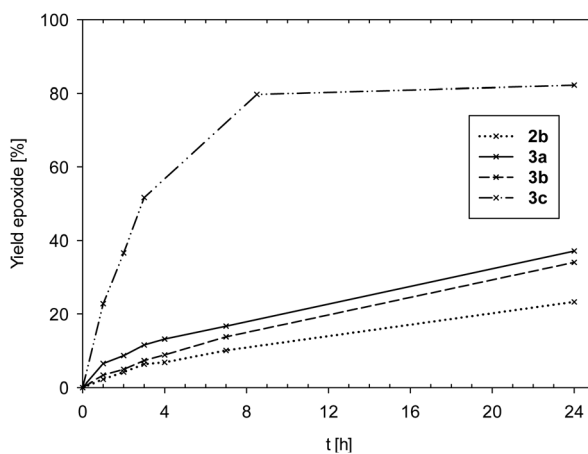


Fig. 5 Comparison of yield of epoxide for complexes **2b** and **3a–c** (**2a** is not shown due to low activity).

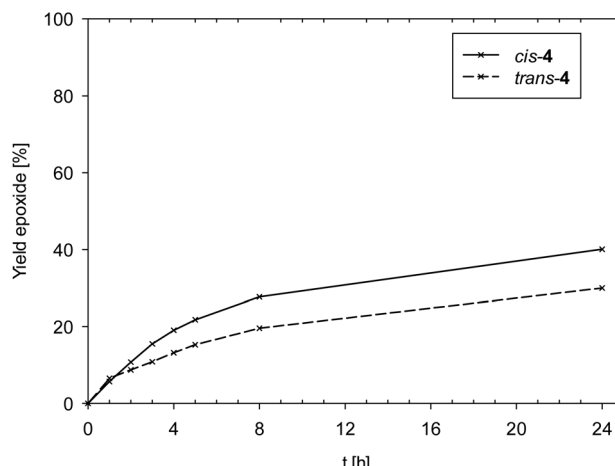


Fig. 6 Yield of epoxide for isomeric complexes *cis/trans*-**4**.

activity (TON = 80) of all seven complexes (Fig. 5). In this case, the same positive effect on catalytic activity was observed as with $[\text{ReOCl}(\text{pyzNO}_2)_2]$.¹⁴ Obviously, the electron-withdrawing property of a nitro group results in enhanced epoxidation activity.

Data in Fig. 6 reveals a slight difference in catalytic performance of isomeric complexes *cis*- and *trans*-**4**, with *cis*-**4** (TON = 40) performing slightly better compared to *trans*-**4** (TON = 30).

With the results from epoxidation catalysis in hand, a potential correlation to structural and spectroscopic data can be probed. Table 6 shows a summary of such data together with TONs in cyclooctene epoxidation. By comparing spectroscopic data of complexes **3a–c** and *cis/trans*-**4** no obvious correlation however between electronic properties and catalyst activity can be drawn.^{12,22} Neither the $\text{Re}=\text{O}$ IR absorption frequency nor the $\text{Re}=\text{O}$ bond lengths show a clear trend correlating to epoxidation activity. For example, *cis*-**4** and **3c** show similar $\text{Re}=\text{O}$ IR absorptions (957 vs. 963 cm^{-1}), but very different activities in epoxidation (TON 40 vs. 80). Similarly, the $\text{Re}=\text{O}$ bond distance of **3c** does not vary considerably from the other six $\text{Re}=\text{O}$ bond distances. Nevertheless, **3c** is the most active epoxidation catalyst tested in this series. The

Table 6 Comparison of selected analytical and epoxidation data for complexes **2a–b**, **3a–c** and *cis/trans*-**4**

	$\nu(\text{C}=\text{N})$ [cm^{-1}]	$\nu(\text{Re}=\text{O})$ [cm^{-1}]	$\lambda_{\text{max}}(\varepsilon)^a$ [μ]	$d(\text{Re}=\text{O})$ [\AA]	$E_{1/2}^b$ [V]	TON ^b
2a^b	1611	962	710 (73)	1.690(7)	Irr. ^c	<10
2b^b	1609	969	580 (56)	1.6801(16)	Irr. ^c	23
3a	1604	955	635 (69) ^b	1.682(6)	0.642	37
3b^b	1582	955	660 (65)	1.757(4)	0.613	34
3c^b	1588	963	670 (85)	1.719(4)	0.922	80
<i>trans</i> - 4²²	1630	972	665 (87)	1.693(2)	0.582	30
<i>cis</i> - 4¹²	1620	957	650 (69)	1.689(8)	0.576	40

^a In CH_2Cl_2 , ε = molar extinction coefficient [$\text{dm}^{-3} \text{ mol}^{-1} \text{ cm}^{-1}$]. ^b This work. ^c Only irreversible redox waves observed.

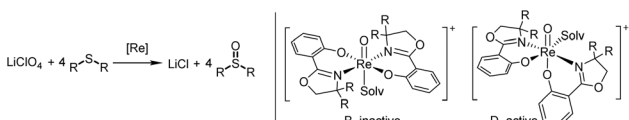


only property of **3c** that is significantly different compared to the other six complexes is the measured redox potential $E_{1/2}$ of 0.922 V. This seems to indicate a more active catalyst if an electron poor rhenium center is present. The similarly active catalyst $[\text{ReOCl}(\text{pyzNO}_2)_2]$ also showed a similar high redox potential $E_{1/2}$ of 0.992 mV.¹⁴

To summarize, stereoisomers as in *cis/trans*-**4** do not play a significant role in epoxidation activity. The observed differences in electronic and steric properties are most likely too small to cause a significant difference in catalytic activity. Electron-withdrawing substituents seem to have a beneficial effect on epoxidation, as both $[\text{ReOCl}(\text{dmozNO}_2)_2]$ **3c** as well as the previously published complex $[\text{ReOCl}(\text{pyzNO}_2)_2]$ showed enhanced catalytic activity.¹⁴ These results indicate that an electron-deficient rhenium center results in higher catalyst activity and must therefore facilitate the oxygen atom transfer from TBHP to the olefin. The exact mode of interaction between the rhenium center and TBHP remains unclear at this point. The redox potential $E_{1/2}$ might have predictive power concerning catalyst activity.

Perchlorate reduction

Complexes **2a–b**, **3a–c** and *cis/trans*-**4** were tested in the challenging reduction of perchlorate to chloride, with a 3.2 mol% catalyst loading in the presence of four equivalents of the sulfide acceptor SMe_2 (DMS) (Scheme 7). Reactions were conducted in $\text{CD}_3\text{CN}/\text{D}_2\text{O}$ mixtures of 95/5 or 50/50 vol%, and the conversion of SMe_2 to OSMe_2 (DMSO) was monitored by ^1H NMR spectroscopy over 24 h. Whereas the 95/5 vol% mixture is necessary to fully dissolve the LiClO_4 substrate, we were interested if higher water contents in the reaction affect catalyst activity. This could either occur by potential hydrolytic decomposition of the catalyst or coordination of the H_2O molecule to the vacant site on the rhenium thereby inhibiting catalysis. From reaction of **4** with AgOTf ($\text{OTf} = \text{SO}_2\text{CF}_3^-$) it is known that H_2O will coordinate to the resulting cationic oxidorhenium(v) triflate complex. The solid state structure of complex $[\text{ReO}(\text{oz})_2(\text{H}_2\text{O})]\text{OTf}$ revealed the formation of a symmetric *N,N-trans* stereoisomer (isomer B, Scheme 7), with the water oxygen atom coordinated *trans* to the oxido ligand and the **oz** ligands in equatorial position.²³ From DFT calculations it was shown that a symmetric cation B is not catalytically active in perchlorate reduction, as the coordination site *trans* to the oxido ligand is deactivated for perchlorate coordination.¹² The catalytically active species therefore should remain an isomer D (Scheme 7), with the vacant coordination site *cis* to the oxido ligand.



Scheme 7 Left: catalytic perchlorate reduction by oxidorhenium(v) complexes; right: catalytically inactive and active stereoisomers in perchlorate reduction; solv = solvent.

Table 7 Yield of DMSO [%] from catalytic perchlorate reduction after 24 h

DMSO [%]	5 vol% D_2O	50 vol% D_2O
2a–b	0	0
3a	75	32
3b	78	64
3c	48 ^a	0 ^b
<i>cis</i> - 4	33	58
<i>trans</i> - 4	>99 ²²	91

Conditions: 3.2 mol% catalyst, 4 equiv. of DMS, $\text{CD}_3\text{CN}/\text{D}_2\text{O}$, 25 °C.

^a Only partly soluble. ^b Insoluble.

Results are summarized in Table 7. While mono-ligated rhenate complexes **2a–b** are not active, complexes **3a–c** and *cis/trans*-**4** were capable to reduce perchlorate at both water contents (5 and 50 vol%), with the exception of nitro-substituted complex **3c**. Complex **3c** showed complete loss of catalytic activity at 50 vol% water. In this case however, we attribute this to the low solubility of **3c** in aqueous media. In both solvent mixtures, solid **3c** can be observed throughout the 24 h experiment time. Similar to our previous findings in 5 vol% water,¹² *trans*-**4** remains the more active complex also at 50 vol% water (91%), compared to *cis*-**4** (58%). It is interesting to observe though that only for *cis*-**4** the catalytic activity increases with increasing water content (33% at 5 vol% vs. 58% at 50 vol%). At 5 vol% water, **3a** and **3b** show essentially the same catalytic activity (75 and 78% respectively, Table 7). At 50 vol% water however, **3a** shows a significantly decreased activity (75 vs. 32%). With **3b**, the difference is not as pronounced (78 vs. 64%).

For all active complexes, catalyst decomposition can be observed by ^1H NMR spectroscopy, as more and more free ligand is visible over the 24 h reaction time. A discoloration of the initially green solutions points to decomposition to perrhenate.³¹ The inactivity of complexes **2a–b** is consistent to previously tested, neutral mono-ligated complexes.¹² The observed differences in catalytic activity in regard to water content are subject to current investigations in our lab.

Conclusions

Oxidorhenium(v) complexes equipped with phenol-dimethoxazoline ligands remain as a unique class of complexes capable to both catalytically epoxidize cyclooctene and reduce the challenging substrate perchlorate to harmless chloride under mild, aqueous conditions. In olefin epoxidation, stereoisomers do not play a significant role in catalyst activity, as demonstrated by the very similar TONs of *cis/trans*-**4** (40/30). Electron withdrawing substituents rather seem to result in more active catalysts. Nitro-substituted complex **3c** showed the highest activity with a TON of 80 for cyclooctene. This is line with the nitro-substituted complex $[\text{ReOCl}(\text{pyzNO}_2)_2]$, which also proved to be a similarly active epoxidation catalyst.¹⁴ From comparison of spectral and structural data, it seems the redox potential

$E_{1/2}$ obtained from cyclic voltammetry measurements correlates with enhanced activity in epoxidation, in contrast to IR absorptions or bond lengths.

In contrast to epoxidation catalysis, stereoisomers play a vital role for catalyst activity in perchlorate reduction. Here, only *N,N-trans* isomers are active. The formation of such *N,N-trans* isomers is a unique feature of the oxazoline ligand moiety. All related pyrazole based complexes $[\text{ReOCl}(\text{pyzR})_2]$ adopted the *N,N-cis* conformation in the solid state, which also explains their inactivity in perchlorate reduction catalysis.¹⁶ For the observed stereoselective synthesis of complexes **3a–c**, a novel mechanism is proposed, based on the two-step coordination of the respective **HL1a–c** ligands. Coordination of the first ligand gives intermediate oxidorhenate(v) complexes $[\text{ReOCl}_3(\text{L1a–c})]^-$, with a strengthened Re–Cl₂ bond thereby directing the second incoming ligand to form an *N,N-trans* complex. Finally, H₂O seems to play a far more important role in perchlorate catalysis than simply dissolving the perchlorate salt. It potentially can also act as an inhibitor by competing with substrate for the vacant coordination site on rhenium and favoring the formation of inactive cationic stereoisomers. Complexes **3a** and **3b** showed a diminished activity at 50 vol% H₂O compared to 5 vol%, whereas conversion to DMSO actually increased for less active stereoisomer *cis*-**4**. The exact role of H₂O however is subject to ongoing investigations in our lab.

Experimental section

General

The rhenium precursors $[\text{ReOCl}_3(\text{OPPh}_3)(\text{SMe}_2)]^{35}$ and $(\text{NBu}_4)[\text{ReOCl}_4]^{36}$ were prepared according to previously published methods. The ligands **HL1a**,^{27,29} **HL1b**²⁸ as well as complexes **3a**¹² and *cis/trans*-**4**¹² were prepared *via* published routes. Synthesis of **HL1c** can be found in the ESI.† Chemicals were purchased from commercial sources and used without further purification. NMR spectra were recorded with a Bruker Avance (300 MHz) instrument. Chemical shifts are given in ppm and are referenced to residual protons in the solvent. Coupling constants (J) are given in Hertz (Hz). Mass spectra were recorded with an Agilent 5973 MSD – Direct Probe using the EI ionization technique. Samples for infrared spectroscopy were measured on a Bruker Optics ALPHA FT-IR Spectrometer equipped with an ATR diamond probe head. GC-MS measurements were performed on an Agilent 7890 A with an Agilent 19091J-433 column coupled to a mass spectrometer type Agilent 5975 C. Electrochemical measurements were performed under an inert N₂ atmosphere in a glove box in dry acetonitrile (stored over molecular sieve) with a Gamry Instruments Reference 600 Potentiostat using a three electrode setup. Platin was used as working electrode, Pt wire (99.99%) as supporting electrode; the reference electrode was a Ag wire immersed in a solution of 0.01 M AgNO₃ and 0.1 M $(\text{NBu}_4)\text{PF}_6$ in CH₃CN separated from the solution by a Vycor® tip. Supporting electrolyte used was $(\text{NBu}_4)\text{PF}_6$ (0.1 M). Elemental

analyses were carried out using a Heraeus Vario Elementar automatic analyzer at the University of Technology Graz.

X-ray structure determinations

Crystallographic data (excluding structure factors) for **2a**, **2b**, **3a**, **3b**, and **3c** were deposited with the Cambridge Crystallographic Data Center as supplementary publication no. 1895410 (**2a**), 1850856 (**2b**), 1562677 (**3a**), 1562678 (**3b**) and 1562679 (**3c**).†

Epoxidation of cyclooctene

A Heidolph Parallel Synthesizer 1 was used for all epoxidation experiments. In a typical experiment, 2–3 mg of catalyst (1 mol%) were dissolved in 0.5 mL CHCl₃ and mixed with cyclooctene (1 equiv.) and 50 μ L of mesitylene (internal standard) and heated to the respective reaction temperature (50 °C). Then the oxidant (3 equiv.) was added. Aliquots for GC-MS (20 μ L) were withdrawn at given time intervals, quenched with MnO₂ and diluted with HPLC grade ethyl acetate. The reaction products were analysed by GC-MS (Agilent 7890 A with an Agilent 19091J-433 column coupled to a mass spectrometer type Agilent 5975 C), and the epoxide produced from each reaction mixture was quantified *vs.* mesitylene as the internal standard. Experimental error of GC-MS measurements is $\pm 5\%$.

Synthesis of complex $(\text{NBu}_4)[\text{ReOCl}_3(\text{L1a})] 2\text{a}$

Ligand **HL1a** (0.030 g, 0.16 mmol, 1 equiv.) and $(\text{NBu}_4)[\text{ReOCl}_4]$ (0.10 g, 0.16 mmol, 1 equiv.) were dissolved in 20 mL EtOH and stirred at rt for 1 h. The mixture turns green within 5 minutes. After 1 h, a small amount of white precipitate (probably NBu_4Cl) is filtered off and the solvent removed completely. The crude product is a mixture of **2a** and bis-ligated **3a**, which can be separated by dissolving the better soluble **3a** in small amounts of EtOAc, leaving behind analytical pure yellowish-greenish **2a** (62 mg, 52%). Recrystallization from EtOH/EtOAc (1/1 vol%) yielded **2a** as single crystals. ¹H NMR (300 MHz, chloroform-d) δ 7.61 (dd, J = 7.9, 1.8 Hz, 1H), 7.12 (ddd, J = 8.7, 7.1, 1.8 Hz, 1H), 7.00–6.90 (m, 1H), 6.90 (ddd, J = 8.2, 7.1, 1.2 Hz, 1H), 4.51 (s, 2H), 3.35–3.23 (m, 8H), 1.74 (s, 6H), 1.72–1.61 (m, 8H), 1.53–1.38 (m, 8H), 1.00 (t, J = 7.3 Hz, 12H). ¹³C NMR (75 MHz, chloroform-d) δ 136.33, 131.32, 118.80, 116.96, 108.59, 78.98 (CH₂), 73.54, 59.41 (NBu_4^+), 26.78 (Me₂), 24.39 (NBu_4^+), 19.95 (NBu_4^+), 13.90 (NBu_4^+), (two C obscured); ATR-IR $\nu_{\text{max}}/\text{cm}^{-1}$: 2960, 2930, 2871, 1612 (C=N), 1482, 1378, 1323, 1271, 1082, 962 and 955 (Re=O), 879, 860, 756, 616; EI-MS (*m/z*): 497.9 (M⁺ – NBu_4); UV $\lambda_{\text{max}}(\text{CH}_2\text{Cl}_2)/\text{nm}$: 710 ($\epsilon/\text{dm}^3 \text{ mol}^{-1} \text{ cm}^{-1}$ 73); elemental analysis calculated for C₂₇H₄₈Cl₃N₂O₄Re (741.3 g mol⁻¹): C 43.75, H 6.53, N 3.78; found C 42.83, 6.51 H, 3.30 N.

Synthesis of complex $(\text{NBu}_4)[\text{ReOCl}_3(\text{L1b})] 2\text{b}$

Ligand **HL1b** (0.083 g, 0.375 mmol, 1.1 equiv.) and $(\text{NBu}_4)[\text{ReOCl}_4]$ (0.20 g, 0.34 mmol, 1 equiv.) were dissolved in EtOH and stirred at rt for 0.5 h. An intense green color formed moments after dissolution. Upon concentration unreacted

(NBu₄)₂[ReOCl₄] precipitated and was removed by filtration. Removal of solvent yielded crude **2b**. Recrystallization from EtOH/EtOAc (1/1 vol%) yielded **2b** as single crystals (105 mg, 42%). ¹H NMR (300 MHz, CDCl₃) δ 7.30 (dd, *J* = 5.6, 4.1 Hz, 1H), 6.81–6.77 (m, 2H), 4.51 (s, 2H), 3.83 (s, 3H), 3.26–3.15 (m, 8H), 1.74 (s, 6H), 1.65–1.52 (m, 8H), 1.37 (m, 8H), 0.95 (t, *J* = 7.3 Hz, 12H); ¹³C NMR (75 MHz, CDCl₃) δ 166.53, 157.48, 148.69, 124.86, 123.98, 116.77, 109.78, 100.11, 78.91 (CH₂), 73.66, 59.54 (OCH₃), 58.83 (NBu₄⁺), 26.81 (Me₂), 24.25 (NBu₄⁺), 19.83 (NBu₄⁺), 13.89 (NBu₄⁺); ATR-IR ν _{max}/cm⁻¹: 2959, 2933, 1609 (C=N), 1582, 1458, 1379, 1254, 1055, 969 and 957 (Re=O), 845, 737, 670, 567, 435; EI-MS (*m/z*): 528.1 (M⁺ – NBu₄); UV λ _{max}(CH₂Cl₂)/nm: 580 (ϵ /dm³ mol⁻¹ cm⁻¹ 56); elemental analysis calculated for C₂₈H₅₀Cl₃N₂O₄Re (771.3 g mol⁻¹): C 43.60, H 6.53, N 3.63; found C 43.78, H 6.48, N 3.66.

UV-Vis data of complex **3a**. UV λ _{max}(CH₂Cl₂)/nm: 650 (ϵ /dm³ mol⁻¹ cm⁻¹ 70); other analytical data has been previously published.¹²

Synthesis of complex [ReOCl(L1b)₂] 3b

Ligand **HL1b** (0.63 g, 2.85 mmol, 2 equiv.) and precursor [ReOCl₃(OPPh₃)(SMe₂)] (0.93 g, 1.43 mmol, 1 equiv.) was heated under reflux in 30 ml CH₃CN for 3 h. Analytically pure **3b** precipitated upon cooling and was isolated by filtration (495 mg, 51%). Single crystals suitable for X-ray diffraction analysis were obtained from EtOH/EtOAc. ¹H NMR (300 MHz, chloroform-d) δ 7.53 (dd, *J* = 8.3, 1.6 Hz, 1H), 7.34 (dd, *J* = 8.0, 1.6 Hz, 1H), 6.92–6.82 (m, 2H), 6.76 (dd, *J* = 8.0, 1.6 Hz, 1H), 6.67 (t, *J* = 8.1 Hz, 1H), 4.67–4.51 (m, 4H), 3.73 (s, 3H), 3.67 (s, 3H), 2.00 (s, 3H), 1.90 (s, 6H), 1.64 (s, 3H); ¹³C NMR (75 MHz, CDCl₃) δ 150.22, 121.98, 121.33, 118.65, 117.54, 116.48, 115.70, 110.92, 81.89, 79.47, 78.75, 72.92, 55.86 (OCH₃), 55.43 (OCH₃), 27.61, 27.10, 27.07, 25.97 (some C are obscured); ATR-IR ν _{max}/cm⁻¹: 1582 (s, C=N), 1379 (s), 1052 (m), 955 (s, Re=O); EI-MS (*m/z*): 678.2 (M⁺); UV λ _{max}(CH₂Cl₂)/nm: 660 (ϵ /dm³ mol⁻¹ cm⁻¹ 65); elemental analysis calculated for C₂₄H₂₈Cl₂N₂O₇Re (678.15 g mol⁻¹): C 42.51, H 4.16, N 4.13; found C 42.74, H 4.06, N 4.08.

Synthesis of complex [ReOCl(L1c)₂] 3c

Ligand **HL1c** (0.50 g, 2.12 mmol, 2 equiv.) and precursor [ReOCl₃(OPPh₃)(SMe₂)] (0.69 g, 1.06 mmol, 1 equiv.) was heated under reflux in 30 ml CH₃CN for 4 h. Analytically pure **3c** precipitated upon cooling and was isolated by filtration (375 mg, 50%). Single crystals suitable for X-ray diffraction analysis were obtained from DCM/heptane. ¹H NMR (300 MHz, CDCl₃) δ 8.98 (d, *J* = 2.8 Hz, 1H), 8.72 (d, *J* = 2.9 Hz, 1H), 8.24 (dd, *J* = 9.3, 2.9 Hz, 1H), 8.07 (dd, *J* = 9.2, 2.9 Hz, 1H), 6.90 (d, *J* = 9.4 Hz, 2H), 6.74 (d, *J* = 9.2 Hz, 1H), 4.79 (dd, *J* = 8.5, 4.1 Hz, 2H), 4.70 (d, *J* = 8.5 Hz, 1H), 4.60 (d, *J* = 8.5 Hz, 1H), 1.96 (s, 3H), 1.95 (s, 3H), 1.84 (s, 3H), 1.67 (s, 3H); because of the low solubility of **3c** no meaningful ¹³C NMR spectra could be acquired; HSQC (CDCl₃) δ 131.05, 130.26, 128.19, 128.01, 122.44, 119.35, 82.40, 82.24, 79.67, 79.62, 27.15, 27.13, 27.10, 25.86; ATR-IR ν _{max}/cm⁻¹: 1611, 1588 (s, C=N), 1312, 1269 (s, NO₂), 963 (s, Re=O); EI-MS (*m/z*): 708.3

(M⁺); UV λ _{max}(CH₂Cl₂)/nm: 670 (ϵ /dm³ mol⁻¹ cm⁻¹ 85); elemental analysis calculated for C₂₂H₂₂ClN₄O₉Re·0.5CH₂Cl₂ (708.06 g mol⁻¹): C 36.00, H 3.09; N 7.46; found C 36.01; H 2.98; N 7.00.

Conflicts of interest

There are no conflicts to declare.

Acknowledgements

The organizers of the 7th EuCheMS conference on N-ligands in September 2018, Lisbon, where parts of this research was presented, are thankfully acknowledged. Financial support from NAWI Graz is gratefully acknowledged.

Notes and references

- (a) W. A. Herrmann, R. W. Fischer and D. W. Marz, *Angew. Chem., Int. Ed. Engl.*, 1991, **30**, 1638–1641; (b) W. A. Herrmann and M. Wang, *Angew. Chem., Int. Ed. Engl.*, 1991, **30**, 1641–1643.
- (a) R. G. Harms, W. A. Herrmann and F. E. Kühn, *Coord. Chem. Rev.*, 2015, **296**, 1–23; (b) J. Rudolph, K. L. Reddy, J. P. Chiang and K. B. Sharpless, *J. Am. Chem. Soc.*, 1997, **119**, 6189–6190; (c) C. Copéret, H. Adolfsson and K. Barry Sharpless, *Chem. Commun.*, 1997, 1565–1566; (d) C. C. Romão, F. E. Kühn and W. A. Herrmann, *Chem. Rev.*, 1997, **97**, 3197–3246.
- S. Huber, M. Cokoja and F. E. Kühn, *J. Organomet. Chem.*, 2014, **751**, 25–32.
- F. E. Kühn, A. Scherbaum and W. A. Herrmann, *J. Organomet. Chem.*, 2004, **689**, 4149–4164.
- W. A. Herrmann, *J. Organomet. Chem.*, 1995, **500**, 149–173.
- J. W. Kück, R. M. Reich and F. E. Kühn, *Chem. Rec.*, 2016, **16**, 349–364.
- S. Yamazaki, *Org. Biomol. Chem.*, 2007, **5**, 2109–2113.
- (a) W. Adam and C. M. Mitchell, *Angew. Chem., Int. Ed. Engl.*, 1996, **35**, 533–535; (b) T. R. Boehlow and C. D. Spilling, *Tetrahedron Lett.*, 1996, **37**, 2717–2720; (c) P. Altmann, M. Cokoja and F. E. Kühn, *Eur. J. Inorg. Chem.*, 2012, 3235–3239.
- W. A. Herrmann, M. U. Rauch and G. R. J. Artus, *Inorg. Chem.*, 1996, **35**, 1988–1991.
- F. E. Kühn, M. U. Rauch, G. M. Lobmaier, G. R. J. Artus and W. A. Herrmann, *Chem. Ber.*, 1997, **130**, 1427–1431.
- N. Zwettler, J. A. Schachner, F. Belaj and N. C. Mösch-Zanetti, *Inorg. Chem.*, 2016, **55**, 5973–5982.
- J. A. Schachner, B. Terfassa, L. M. Peschel, N. Zwettler, F. Belaj, P. Cias, G. Gescheidt and N. C. Mösch-Zanetti, *Inorg. Chem.*, 2014, **53**, 12918–12928.
- (a) B. Terfassa, J. A. Schachner, P. Traar, F. Belaj and N. C. Mösch-Zanetti, *Polyhedron*, 2014, **75**, 141–145; (b) B. Machura, M. Wolff, D. Tabak, J. A. Schachner and



N. C. Mösch-Zanetti, *Eur. J. Inorg. Chem.*, 2012, 3764–3773;
(c) S. Dinda, M. G. B. Drew and R. Bhattacharyya, *Catal. Commun.*, 2009, **10**, 720–724.

14 N. Zwettler, J. A. Schachner, F. Belaj and N. C. Mösch-Zanetti, *Inorg. Chem.*, 2014, **53**, 12832–12840.

15 B. Machura, M. Wolff, E. Benoist, J. A. Schachner and N. C. Mösch-Zanetti, *Dalton Trans.*, 2013, **42**, 8827–8837.

16 P. Traar, J. A. Schachner, L. Steiner, A. Sachse, M. Volpe and N. C. Mösch-Zanetti, *Inorg. Chem.*, 2011, **50**, 1983–1990.

17 B. Machura, M. Wolff and I. Gryca, *Coord. Chem. Rev.*, 2014, **275**, 154–164.

18 F. E. Kühn, A. M. Santos and W. A. Herrmann, *Dalton Trans.*, 2005, **34**, 2483–2491.

19 W. A. Herrmann, R. W. Fischer, M. U. Rauch and W. Scherer, *J. Mol. Catal.*, 1994, **86**, 243–266.

20 (a) L. F. Veiros, A. Prazeres, P. J. Costa, C. C. Romão, F. E. Kühn and M. J. Calhorda, *Dalton Trans.*, 2006, 1383–1389; (b) J. Morlot, N. Uyttebroeck, D. Agustin and R. Poli, *ChemCatChem*, 2013, **5**, 601–611; (c) M. E. Judmaier, C. Holzer, M. Volpe and N. C. Mösch-Zanetti, *Inorg. Chem.*, 2012, **51**, 9956–9966.

21 J. R. Winkler and H. B. Gray, in *Molecular electronic structures of transition metal complexes*, ed. D. M. P. Mingos, J. P. Dahl and M. Atanasov, Springer, Berlin, 2012, pp. 17–28.

22 M. M. Abu-Omar, L. D. McPherson, J. Arias and V. M. Béreau, *Angew. Chem., Int. Ed.*, 2000, **39**, 4310–4313.

23 J. Arias, C. R. Newlands and M. M. Abu-Omar, *Inorg. Chem.*, 2001, **40**, 2185–2192.

24 L. D. McPherson, M. Drees, S. I. Khan, T. Strassner and M. M. Abu-Omar, *Inorg. Chem.*, 2004, **43**, 4036–4050.

25 M. M. Abu-Omar, *Comments Inorg. Chem.*, 2003, **24**, 15–37.

26 J. Liu, D. Wu, X. Su, M. Han, S. Y. Kimura, D. L. Gray, J. R. Shapley, M. M. Abu-Omar, C. J. Werth and T. J. Strathmann, *Inorg. Chem.*, 2016, **55**, 2597–2611.

27 J. Liu, X. Su, M. Han, D. Wu, D. L. Gray, J. R. Shapley, C. J. Werth and T. J. Strathmann, *Inorg. Chem.*, 2017, **56**, 1757–1769.

28 H. C. Aspinall, O. Beckingham, M. D. Farrar, N. Greeves and C. D. Thomas, *Tetrahedron Lett.*, 2011, **52**, 5120–5123.

29 P. G. Cozzi, C. Floriani, A. Chiesi-Villa and C. Rizzoli, *Inorg. Chem.*, 1995, **34**, 2921–2930.

30 M. Hoogenraad, K. Ramkisoensing, S. Gorter, W. L. Driessens, E. Bouwman, J. G. Haasnoot, J. Reedijk, T. Mahabiersing and F. Hartl, *Eur. J. Inorg. Chem.*, 2002, 377–387.

31 G. M. Lobmaier, G. D. Frey, R. D. Dewhurst, E. Herdtweck and W. A. Herrmann, *Organometallics*, 2007, **26**, 6290–6299.

32 (a) S. Gatto, T. I. A. Gerber, G. Bandoli, J. Perils and J. G. H. Du Preez, *Inorg. Chim. Acta*, 1998, **269**, 235–240; (b) C. Bolzati, F. Tisato, F. Refosco, G. Bandoli and A. Dolmella, *Inorg. Chem.*, 1996, **35**, 6221–6229; (c) S. M. Harben, P. D. Smith, R. L. Beddoes, D. Collison and C. D. Garner, *J. Chem. Soc., Dalton Trans.*, 1997, 2777–2784; (d) H. Luo, S. J. Rettig and C. Orvig, *Inorg. Chem.*, 1993, **32**, 4491–4497; (e) M. Shivakumar, S. Banerjee, M. Menon and A. Chakravorty, *Inorg. Chim. Acta*, 1998, **275–276**, 546–551; (f) J. D. G. Correia, Â. Domingos, I. Santos, C. Bolzati, F. Refosco and F. Tisato, *Inorg. Chim. Acta*, 2001, **315**, 213–219; (g) E. J. de Souza, V. M. Deflon, A. G. de, A. Fernandes, S. S. Lemos, A. Hagenbach and U. Abram, *Inorg. Chim. Acta*, 2006, **359**, 1513–1518.

33 A. Sachse, N. C. Mösch-Zanetti, G. Lyashenko, J. W. Wielandt, K. Most, J. Magull, F. Dall'Antonia, A. Pal and R. Herbst-Irmer, *Inorg. Chem.*, 2007, **46**, 7129–7135.

34 C. C. van Kirk, V. M. Béreau, M. M. Abu-Omar and D. H. Evans, *J. Electroanal. Chem.*, 2003, **541**, 31–38.

35 B. D. Sherry, R. N. Loy and F. D. Toste, *J. Am. Chem. Soc.*, 2004, **126**, 4510–4511.

36 R. Alberto, R. Schibli, A. Egli, P. August Schubiger, W. A. Herrmann, G. R. J. Artus, U. Abram and T. A. Kaden, *J. Organomet. Chem.*, 1995, **493**, 119–127.

